

Transient Inhibition of the Mediodorsal Thalamus During Early Adolescence Induces Hypofrontality and Social Memory Deficits in Young Adulthood

Sha-Sha Yang, Quansheng He, Xinyang Gu, Shoupei Liu, Wei Ke, Liang Chen, Bo Li, Yousheng Shu, and Wen-Jun Gao

ABSTRACT

BACKGROUND: Dysconnectivity between the mediodorsal thalamus (MD) and medial prefrontal cortex (mPFC) during adolescence is linked to developmental and psychiatric disorders, as well as social behavioral deficits. However, the precise mechanisms that underlie these impairments remain elusive.

METHODS: We transiently inhibited MD activity with inhibitory DREADDs (HM4Di) in adolescent mice. Then, we examined the social behavior performance by a three-chamber social behavioral paradigm and neural excitability in both MD and mPFC neurons in adulthood with multiple approaches.

RESULTS: We revealed that this transient MD inhibition during adolescence led to impaired social memory in adulthood. The neuronal excitability of both MD and mPFC excitatory neurons decreased. Meanwhile, excitatory synaptic transmission in excitatory pyramidal neurons in the mPFC was impaired. In vivo calcium imaging showed a persistent reduction of general calcium activity in the mPFC. Unexpectedly, there were significant alterations in intrinsic excitability and synaptic function changes in somatostatin but not in parvalbumin interneurons.

CONCLUSIONS: Our findings provide insights into the role of MD input activity in shaping the circuit and functional maturation of the mPFC that is critical for the normal development of social memory and abnormal deficits in psychiatric disorders.

<https://doi.org/10.1016/j.bpsgos.2025.100486>

The medial prefrontal cortex (mPFC) is a hub of social brain networks, and deficits of prefrontal cortical functions have been implicated in multiple psychiatric disorders (1–5), which consistently show impairments in social cognition (6–10). The mPFC undergoes protracted postnatal development, and disruption of its input activity during a critical developmental window is likely a mechanistic substrate of mPFC-dependent cognitive deficits observed in psychiatric disorders (11–15). Therefore, elucidating the association between developmental deficits in prefrontal circuits and social cognitive impairments is essential for understanding their underlying pathological mechanisms.

The mediodorsal thalamus (MD) provides a large volume of excitatory inputs to the mPFC (16–18), and the rodent mPFC is largely defined by these projections (19,20). While the causal relationships between MD projections and functional deficits of the mPFC have been addressed in animal studies (21), the precise mechanisms of MD-influenced mPFC maturation, both at the single-cell and circuit levels, especially during development, remains unclear. Recently, a mouse study revealed that a month-long thalamic inhibition during adolescence caused long-lasting cognitive deficits in adulthood, which were associated with decreased prefrontal neural activities (22). However, the influence of adolescent MD disruption on social behaviors remains untested. Previous studies have implicated

the MD-mPFC circuit in social behaviors in adult rodents, with acute MD inhibition disrupting sociability through the regulation of excitation/inhibition (E/I) balance (23). Nevertheless, whether MD activity disruption during adolescent development affects social behaviors and its association with PFC dysfunction remains unclear.

Thus, in the current study, we investigated the effects of MD input activity during adolescence on the development of different subtypes of neurons in the mouse mPFC by using in vivo chemogenetic inhibition, combined with whole-cell patch clamp recording, in vivo 3-photon imaging, and behavioral testing. Specifically, we used inhibitory chemogenetics to transiently suppress MD activity for 5 consecutive days during early adolescence (postnatal day 35 [P35] to P42), a typical time window equivalent to drug-induced abnormal development of the mPFC (24). Our data revealed that transient MD inhibition during early adolescence led to impaired social memory in adulthood, which was associated with decreased neural excitability in both MD and mPFC excitatory pyramidal neurons (PNs), suppressed prefrontal neural activity, and showed subpopulation-specific changes in somatostatin (SST) but not parvalbumin (PV) interneurons (INs). Our findings provide insights into the critical role of MD input activity in shaping the adolescent maturation of mPFC circuitry and function,

which is essential for the normal development of social memory and for understanding the mechanisms of social deficits in hypofrontality-associated psychiatric disorders.

METHODS AND MATERIALS

The methods have been briefly described and details can be found in the [Supplement](#).

Animals

All mice were purchased from Jackson Laboratory, including C57BL/6J (#000664), SST-Cre (#013044), PV-Cre (#008069), and Ai9-tdTomato (#007909) mice. SST-Cre or PV-Cre and Ai9-tdTomato mice were in-house bred, and heterozygous SST-Cre::Ai9 and PV-Cre::Ai9 mice were used. On P40 to P43 and P60 to P70, 2 groups (saline and clozapine *N*-oxide [CNO]) of mice were used for physiological recording. The 3-chamber test was conducted during P60 to P70. The animals were maintained under standard housing conditions with food and water available ad libitum according to the protocol approved by the Institutional Animal Care and Use Committee of Drexel University and the Department of Laboratory Animal Science at Fudan University.

Viral Vector Injection and CNO Treatment

To inhibit MD during adolescence, AAV9-CaMKII α -hM4D(Gi)-mCherry (Addgene) or AAV9-CaMKII α -hM4D(Gi)-GFP (OBiO) (300 nL, 50 nL/minute) were bilaterally injected into the MD at P20. Prefrontal SST- or PV-INs were labeled with tdTomato in SST-Cre::Ai9 and PV-Cre::Ai9 mice. Animals for in vivo calcium imaging were simultaneously injected with AAV9-hSyn-GCaMP6s (OBiO) into the mPFC. Two weeks following the viral injection, mice were injected with saline or CNO (3 mg/kg, 0.5 mg/mL, intraperitoneally) twice per day (minimum 8-hour intervals) for 5 consecutive days from P35 to P42.

Three-Chamber Test

Adult male mice (P60–P70) were tested as described in our previous publication (25). Animals were habituated in the center chamber for 5 minutes. In phase 1, a stranger mouse was put into the left or right enclosure (systematically alternated) to test social preference. The test mouse was allowed to explore the 3 chambers for 10 minutes. Then, the mouse was home caged for a 10-minute intertrial interval. In phase 2, a novel stranger mouse was placed in the empty enclosure from phase 1. The test mouse was again placed back to the center chamber to start the 10-minute free exploration for social novelty test. Both familiar and novel mice were adult male mice (P60–P70) to avoid sex and age effects on social behaviors of the test mice. The behavioral activity of mice was videotaped. The duration of sniffing and exploration of the chambers were measured using the EthoVisionXT behavior tracking system (Noldus).

Slice Preparation, Ex Vivo Electrophysiology, and Data Analysis

Both male and female mice were included. Mice were anesthetized and decapitated. Brains were removed, and coronal slices containing the mPFC or MD regions were cut at 300 μ m using Leica VT1200S. They were then incubated at 36 $^{\circ}$ C for 40 minutes before being maintained at room temperature until

recording. Slices were placed in a submerged recording chamber (35–36 $^{\circ}$ C) filled with oxygenated artificial cerebrospinal fluid.

Whole-cell recordings were performed on the MD, layer 3 PNs, and SST+ or PV+ tdTomato-labeled cells in the pre-limbic area (PL) of the mPFC (Axon MultiClamp 700B). SST- and PV-INs labeled with tdTomato were identified and recorded under infrared light with differential interference contrast. The resistance of the recording glass pipette was 4 to 6 M Ω when measured with the intracellular solution. The access resistance during recording was 15 to 20 M Ω and was auto-compensated. Data were excluded when the change of series resistance exceeded 20%. The signals were digitized at 10 kHz and low-pass filtered at 1 kHz.

Intrinsic properties and E/I ratio were characterized with K+gluconate-based intracellular solution filled pipette. Under current-clamp mode, we injected a series of current steps into the membrane (–350 pA to 350 pA, 50 pA increment) to measure the resting membrane potential (RMP), voltage sag, tau, input resistance (IR), and action potential (AP) properties, including rheobase, frequency, AP half-width, amplitude, and afterhyperpolarization potential. Under voltage-clamp mode, the cell was held at –60 mV to record evoked excitatory postsynaptic currents (EPSCs) and 0 mV for evoked inhibitory postsynaptic currents (IPSCs), the reversal potential for AMPA receptor (AMPA) and GABA_A (gamma-aminobutyric acid A) receptor mediated currents, respectively. The E/I ratio was calculated with the amplitude of AMPA-EPSCs/GABA-IPSCs.

Evoked EPSCs were tested with a glass pipette filled with a cesium hydroxide-based intracellular solution. A glass pipette filled with artificial cerebrospinal fluid was placed in layer 2/3 of the mPFC, ~300 μ m from the recording cell, and paired-pulse stimulation (10 Hz, 0.5 ms duration) was given to induce synaptic transmission. Under voltage-clamp mode, AMPA-EPSCs were recorded with the cell held at –60 mV, while NMDA receptor (NMDAR) mediated NMDA-EPSCs were recorded at +60 mV. Picrotoxin (50 μ M) was bath applied throughout the recording to block GABA_A receptor-mediated transmission. NBQX (10 μ M) was bath applied to block AMPARs after recording AMPA-EPSCs to isolate NMDA-EPSCs.

The acquired data were processed using Clampfit 10 and MATLAB (version 2019a; The MathWorks, Inc.). Neurons with depolarized RMPs (> –52 mV) were discarded. IR was calculated from the –100 pA current step. Voltage sag was measured from the –300 pA step. The frequency-current curve was plotted with the current step as input and the AP frequency of each current step as output. The AMPA/NMDA ratios were calculated by measuring the amplitude of the first AMPA- and NMDA-EPSCs. Paired-pulse ratios (PPRs) of both AMPA- and NMDA-EPSCs were measured by dividing the second amplitude by the first amplitude. The current decay time (63%) was measured from the EPSC at first pulse.

In Vivo 3-Photon Imaging and Data Analysis

In vivo imaging of the mPFC was performed using a home-built 3-photon laser-scanning microscope with a femtosecond laser (Ligh Conversion) tuned to 1300 nm for imaging of cells expressing GCaMP6s. Both male and female mice were included. Animals were head fixed under the objective lens using a custom-designed headbar. All mice were habituated to

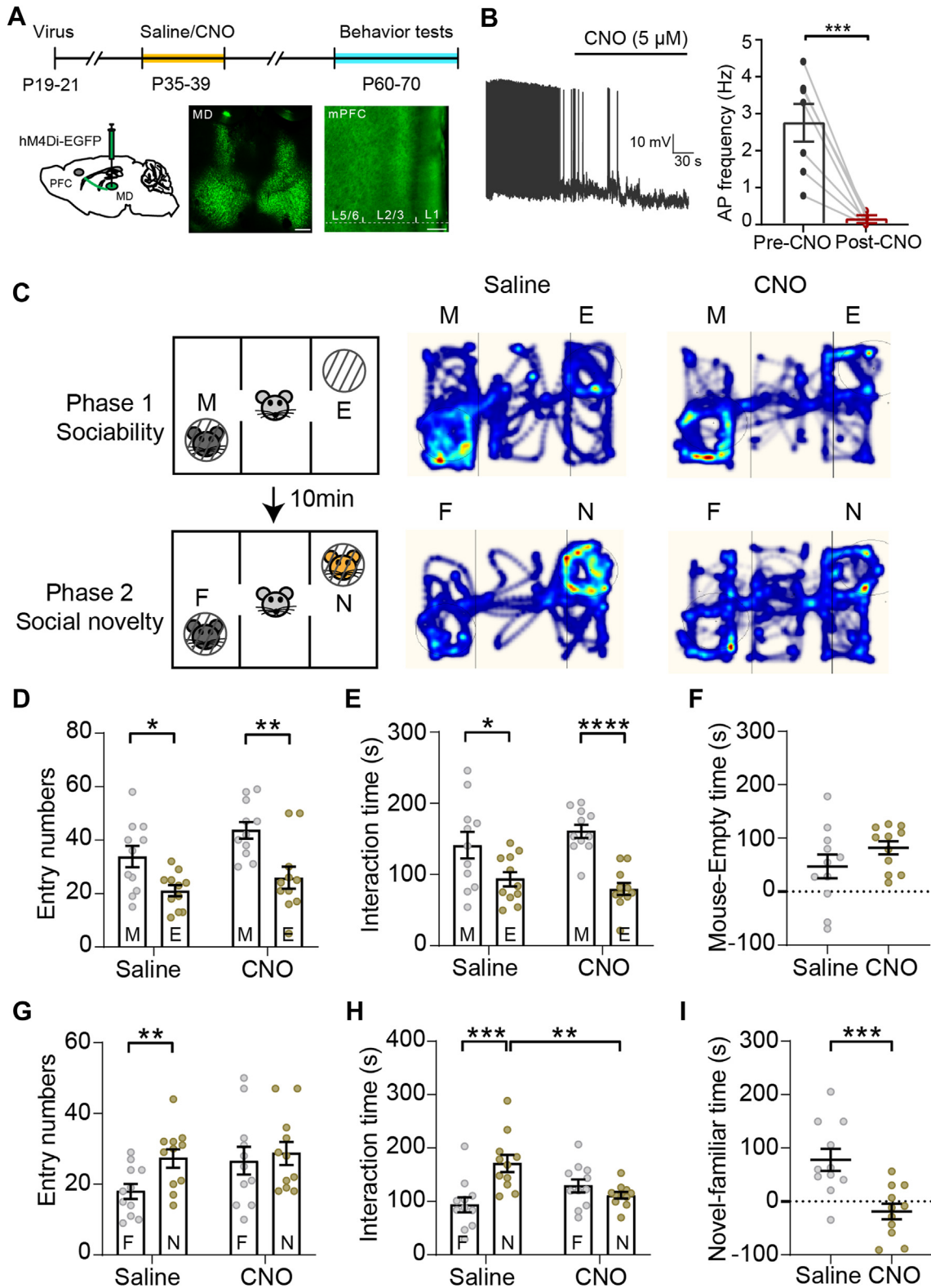


Figure 1. Transient MD inhibition in early adolescence leads to long-lasting impairment of social memory. **(A)** Top: Timeline of the experimental procedure. HM4D(Gi)-expressing viral vectors were injected into the MD region on P19 to P21. Saline or CNO (3 mg/kg, intraperitoneally) was injected twice daily from P35 to P39. Behavioral tests were carried out from P60 to P70. Bottom: Virus expression was restricted into the MD and EGFP-labeled thalamic axon terminals in

the headbar and microscope for 7 days. Recordings were performed in awake mice. Time-series movies of GCaMP6s+ neurons were acquired at a frame rate of 3.51 Hz. The duration of each focal plane movie was 925.93 seconds (6500 frames) to track spontaneous calcium transients of prefrontal neurons located at 900 to 1200 μm below the dura.

Image analysis was performed offline with suite2p software. The time series was corrected for X-Y axis motion. Then, a machine learning-based denoise program was used to reduce background noise (26). The denoised tiff images were imported into suite2p for cell segmentation, and regions of interest (ROIs) were semimanually selected. The detection of calcium transients of individual ROIs was performed automatically using custom-written MATLAB scripts. Active ROIs were ones with at least 1 calcium transient. The baseline fluorescence was defined as the lowest 20% of averaged gray values at every time point in each ROI. $\Delta F/F$ signals were computed as the difference between each fluorescence time point and the mean of the detected fluorescence baseline divided by the mean of the baseline. A qualified calcium transient event was defined as the $\Delta F/F$ at the peak being 3 SDs larger than the baseline mean. Events smaller than 3 SDs from the baseline were excluded from the statistical analysis. The frequency (spikes/min), amplitude, and duration of calcium transient events were measured and analyzed using custom MATLAB scripts.

Histology

After completing the recording, slices from both MD and mPFC were transferred into 4% paraformaldehyde for 30 minutes and then mounted on slides. The expression of hM4D in the MD and GCaMP6s in the mPFC was confirmed by a Nikon C1 confocal microscope.

Statistical Analysis

Statistical analysis was performed using SPSS (version 23; IBM Corp.), with data presented as mean \pm standard error. For parametric data, we first did the Shapiro-Wilk normality test. For datasets that passed the test, 2-way analysis of variance (ANOVA, treatment \times time point) was used to examine the difference between the saline and CNO groups at 3 different time points. If the interaction effect was significant, Tukey's multiple comparisons test was used for group comparisons. A Student's *t* test was conducted when there was an insignificant interaction effect. For these datasets that failed the normality test or had significant variance, the Mann-Whitney test was used for between-group comparison. The Mann-Whitney test was conducted for nonparametric analysis, including noncontinuous and 0-containing datasets.

RESULTS

Transient MD Inhibition in Adolescence Impairs Social Memory in Adulthood

To inhibit thalamic activity during adolescence, we injected the inhibitory designer receptor hM4D-expressing AAV (adeno-associated virus) (AAV-DREADDs-hM4Di) into the MD in P19 to P21 mice (Figure 1A). Mice with virus expression restricted to the MD were used for further experiments (Figure 1A). To determine the efficacy of the hM4Di receptors, we performed patch clamp recordings on MD neurons from a separate batch of mice 2 weeks after viral injection. The designer receptor-specific ligand CNO (5 μM) was bath applied to the MD slices. APs evoked by depolarized current injection were significantly blocked by the application of CNO (Figure 1B).

Then, we examined the long-term effects of transient MD inhibition during adolescence (P39–P42) on social behaviors using a 2-phase, 3-chamber paradigm (Figure 1C). The behavioral test was performed during P60 to P70. Behavioral tests were performed in male mice. During phase 1, namely the sociability test, both saline- and CNO-treated mice could distinguish between a mouse and an empty chamber, as shown by more frequent entries (Figure 1C, D) and more time spent (Figure 1C, E) in the social interaction zone than in the empty chamber. Differences in time spent in each chamber were comparable between saline- and CNO-treated animals (Figure 1F), suggesting that MD inhibition during adolescence does not affect social preference in adulthood.

During phase 2, namely the social novelty test, saline-treated mice made more frequent entries and spent more time in the novel mouse interaction zone than that of the familiar mouse (Figure 1C, G, H). However, CNO-treated mice entered the interaction zone of familiar and novel mice at comparable frequencies (Figure 1C, G) and durations (Figure 1H). The differences in time spent between novel and familiar mice in the saline group were significantly higher than in the CNO group (Figure 1I). These results suggest that transient inhibition of thalamic activity during adolescence induces persistent social memory deficits in adulthood.

Transient MD Inhibition in Early Adolescence Decreases the Excitability of MD and PFC Neurons in Adulthood

Then, we tested both short- and long-term effects of 5-day adolescent MD inhibition on the excitability of the MD-PFC circuit. Ex vivo electrophysiological recordings of the MD

the prelimbic region of the medial PFC. (B) Verification of the efficacy of hM4D receptors in MD neurons by whole-cell patch clamp recordings ($n = 7$ cells, Mann-Whitney test, $U = 0$, $p = .0006$). (C) Schematic of the 3-social chamber social interaction task and heatmap indication of the amount of time spent in each chamber. The behavioral paradigm consists of a social preference trial and a social novelty trial, with 10-minute intervals. (D) Interaction numbers with mouse and empty chambers during the sociability test for mice in the saline group ($n = 11$ mice, Mann-Whitney test, $U = 24$, $p = .0164$) and CNO-treated mice ($n = 11$ mice, Mann-Whitney test, $U = 16.5$, $p = .0026$). (E) Interaction time with mouse and empty chambers during the sociability test [2-way ANOVA, $F_{\text{treatment}(1,40)} = 27.18$, $p < .0001$; post hoc, saline, $t_{19} = 2.214$, $p = .0386$; CNO, $t_{23} = 6.466$, $p < .0001$]. (F) Interaction time differences between the mouse and the empty chamber in the saline and the CNO group are similar (*t* test, $t_{20} = 1.369$, $p = .186$). (G) Interaction number with familiar and novel mice from saline ($n = 11$ mice, Mann-Whitney test, $U = 22.0$, $p = .0098$) and CNO ($n = 11$ mice, Mann-Whitney test, $U = 52.50$, $p = .6169$) groups. (H) Interaction time with familiar and novel mice from saline and CNO groups [2-way ANOVA, $F_{\text{interaction}(1,40)} = 14.40$, $p = .0005$; multiple comparisons test, saline: familiar vs. novel, $t = 6.128$, $p = .0005$; novel: saline vs. CNO, $t = 4.775$, $p = .0086$]. (I) The difference in time spent with novel vs. familiar mice (*t* test, $t_{20} = 3.812$, $p = .0011$). * $p < .05$, ** $p < .01$, *** $p < .001$, **** $p < .0001$. ANOVA, analysis of variance; CNO, clozapine *N*-oxide; E, empty; EGFP, enhanced green fluorescent protein; F, familiar; ITI, intertrial interval; M, mouse; MD, mediodorsal thalamus; N, novel; P, postnatal day; PFC, prefrontal cortex.

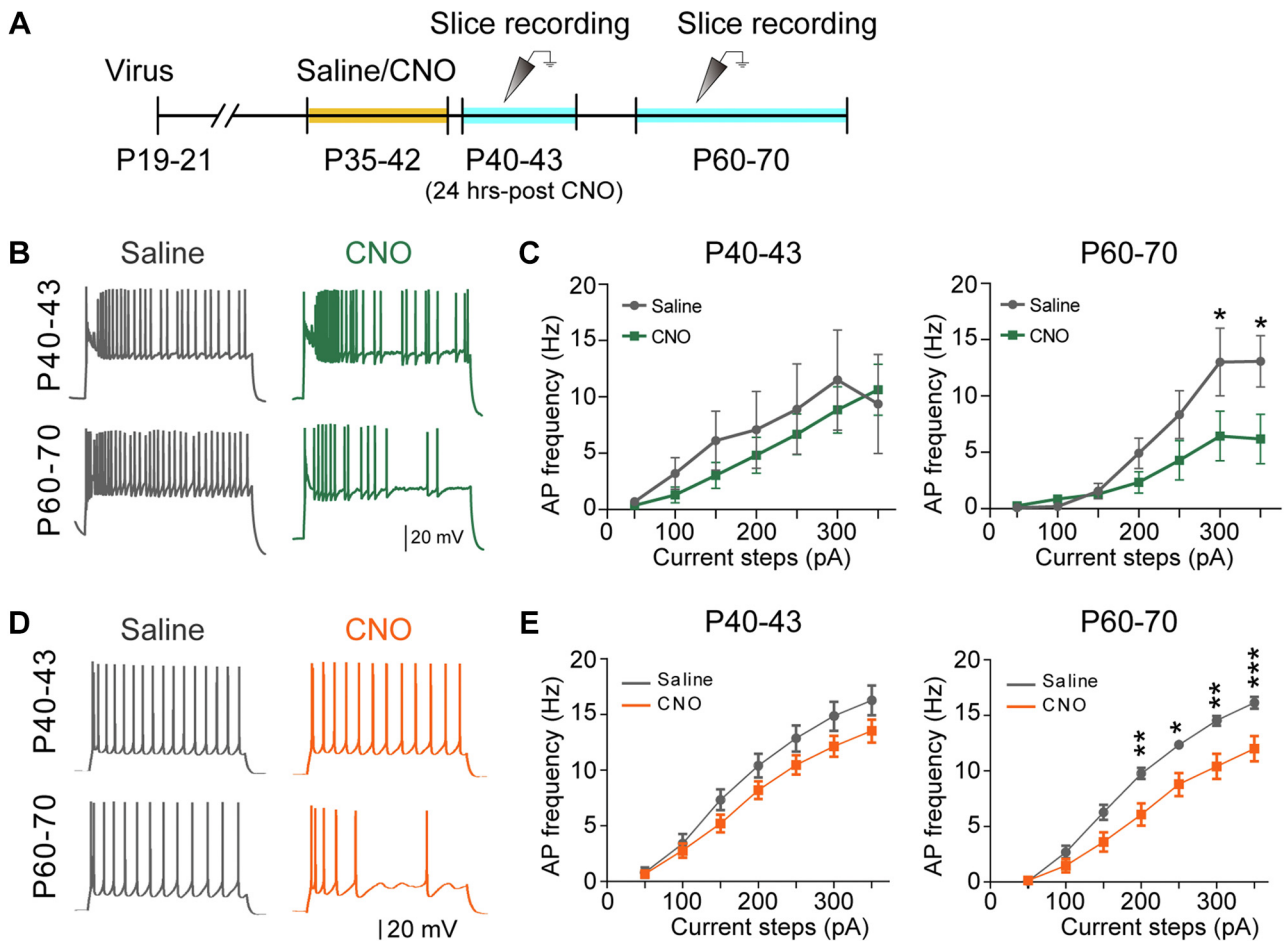


Figure 2. Adolescent MD inhibition leads to long-lasting impairment of excitability in both MD neurons and prefrontal PNs. **(A)** The timeline of the experimental procedure. CNO was administered for 5 consecutive days from P35 to P42. Ex vivo slice recordings were conducted on P40 to P43 and P60 to P70. **(B)** Representative traces of APs recorded in MD neurons (300 pA, 1500 ms in duration). **(C)** Curves of AP frequency plotted against input current on P40 to P43 and P60 to P70 [P40–P43: saline, $n = 16$ cells, CNO, $n = 25$ cells, mixed model 2-way ANOVA, $F_{\text{treatment}(1,39)} = 0.3833$, $p = .5394$; P60–P70: saline, $n = 21$ cells; CNO, $n = 18$ cells; $F_{\text{interaction}(6,222)} = 2.821$, $p = .0115$. Sidak’s multiple comparison test, 300 pA, $t = 2.886$, $p < .05$; 350 pA, $t = 3.028$, $p < .05$]. **(D)** Representative traces of voltage responses to step current injections (200 pA, 1500 ms in duration) in PNs in the medial prefrontal cortex. **(E)** Curves of AP frequency in PNs plotted against input currents on P40 to P43 and P60 to P70 [P40–P43: saline, $n = 20$ cells, CNO, $n = 26$ cells, mixed model 2-way ANOVA, $F_{\text{interaction}(7,308)} = 2.260$, $p = .0295$; $F_{\text{treatment}(1,44)} = 3.102$, $p = .0852$; P60–P70: saline, $n = 16$ cells; CNO, $n = 16$ cells; $F_{\text{interaction}(7,210)} = 5.121$, $p < .0001$; multiple comparison test: 200 pA, $t = 3.298$, $p < .01$; 250 pA, $t = 3.217$, $p < .05$; 300 pA, $t = 3.787$, $p < .01$; 350 pA, $t = 4.031$, $p < .0001$]. * $p < .05$, ** $p < .01$, *** $p < .001$. ANOVA, analysis of variance; AP, action potential; CNO, clozapine *N*-oxide; MD, mediodorsal thalamus; P, postnatal day; PN, pyramidal neuron.

were performed in adolescents (P40–P43) and adults (P60–P70), respectively. Most of the recordings were performed in slices collected from male mice, and a small fraction of cells were collected from female mice in this and the sections mentioned below (see Table S2). We tested the neuronal excitability by depolarizing the cell to induce APs. The results showed changes in excitability in adulthood in both MD and prefrontal PNs. The AP frequency of MD neurons was not affected in adolescent mice (Figure 2B, C). In adults, the AP frequency of MD neurons was significantly decreased at 300 pA and 350 pA current steps (Figure 2B, C), suggesting a reduction of excitability of MD neurons.

Next, we tested the excitability changes of PNs located in layer 2/3 of the PL of the mPFC. We found that layer 2/3 PNs

did not show excitability deficits in adolescents (Figure 2D, E). However, in adults, AP frequency was significantly reduced from 150 pA to 350 pA current steps (Figure 2D, E). This finding is consistent with the changes seen in the MD, which suggests that 5-day inhibition of the thalamus during early adolescence is sufficient to induce a long-lasting changes in MD-PFC circuit function.

Transient MD Inhibition in Adolescence Alters Synaptic Properties in PNs in the PFC

In the neocortex, thalamocortical connections are subject to rapid plasticity changes (27). AMPA and NMDA receptors are 2 primary glutamatergic receptors in excitatory synapses. The

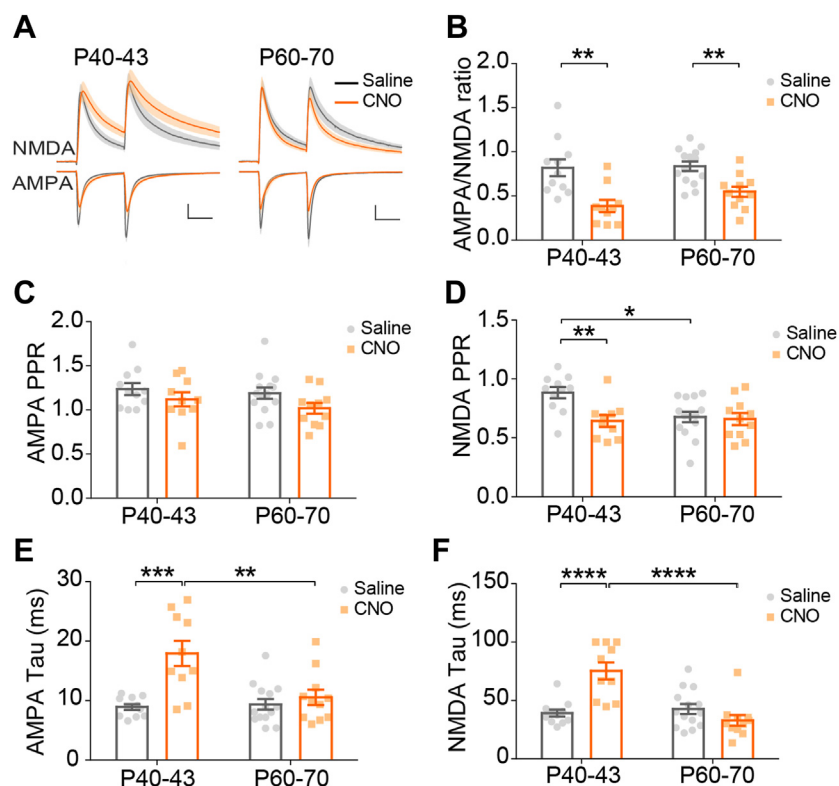


Figure 3. Adolescent mediadorsal thalamus inhibition leads to long-lasting changes in synaptic properties of PNs in the medial prefrontal cortex. **(A)** Representative traces show evoked AMPA- (holding potential V_h at -60 mV) and NMDA-EPSCs ($V_h + 60$ mV) in PNs. Scale bar = 50 pA, 50 ms. **(B)** The ratio of AMPA- to NMDA-EPSC amplitudes in PNs on P40 to P43 (saline, $n = 11$ cells; CNO, $n = 10$ cells) and P60 to P70 groups [saline, $n = 14$ cells; CNO, $n = 11$ cells]. Two-way analysis of variance, $F_{treatment(1,42)} = 26.60$, $p < .0001$; post hoc test, P40–P43: saline vs. CNO, $t_{23} = 3.613$, $p = .0019$; P60–P63: saline vs. CNO, $t_{23} = 3.626$, $p = .0014$. **(C)** The PPRs of AMPA-EPSCs [$F_{interaction(1,42)} = 0.1610$, $p = .6903$; $F_{treatment(1,42)} = 4.406$, $p = .0419$; post hoc test, P40–P43: $t_{19} = 1.236$, $p = .2780$; P60–P65: $t_{19} = 1.899$, $p = .0702$]. **(D)** The PPRs of NMDA-EPSCs [$F_{interaction(1,42)} = 5.271$, $p = .0267$; multiple comparisons, P40–P43: saline vs. CNO, $t = 4.774$, $p = .0083$; saline: P40–P43 vs. P60–P70, $t = 4.443$, $p = .0157$]. **(E)** The time constant decays (tau) of AMPA-EPSCs [$F_{interaction(1,42)} = 9.628$, $p = .0034$; multiple comparisons, P40–P43: saline vs. CNO, $t = 6.8510$, $p = .0001$; CNO: P40–P43 vs. P60–P70, $t = 5.6320$, $p = .0015$]. **(F)** The time constant decays (tau) of AMPA- and NMDA-EPSCs [$F_{interaction(1,42)} = 92.41$, $p < .0001$; P40–P43: saline vs. CNO, $t = 7.004$, $p < .0001$; CNO: P40–P43 vs. P60–P70, $t = 8.217$, $p < .0001$]. * $p < .05$, ** $p < .01$, *** $p < .001$, **** $p < .0001$. CNO, clozapine *N*-oxide; EPSC, excitatory postsynaptic current; P, postnatal day; PN, pyramidal neuron; PPR, paired-pulse ratio.

ratio of AMPA/NMDA critically regulates synaptic plasticity, neural development, and network activity and is subject to change throughout development (28,29). However, the developmental change in the AMPA/NMDA ratio of prefrontal PNs and the contribution of MD inputs to synaptic maturation is unclear. We recorded the AMPA- and NMDA-EPSCs in PNs. The amplitude of evoked EPSCs was measured to calculate the AMPA/NMDA ratio. We found that MD inhibition in adolescence caused a long-lasting decrease in AMPA/NMDA ratio (Figure 3A, B), suggesting a synaptic downscaling of AMPARs during development in the mPFC. We also measured the PPR and the tau of both AMPA- and NMDA-EPSCs. The PPR of AMPA-EPSCs was unchanged (Figure 3C), suggesting that neither AMPAR sensitivity nor presynaptic vesicle release was affected. In contrast, the PPR of NMDA-EPSCs in adolescence was decreased following the 5-day CNO treatment (Figure 3D). The tau of both AMPA and NMDA-EPSCs was increased transiently in adolescence and returned to the saline control level in adulthood (Figure 3E, F). Together, these results suggest that transient inhibition of MD in adolescence decreased the capability of AMPA receptors-mediated synaptic transmission in PFC in adulthood.

Transient MD Inhibition in Adolescence Decreases Calcium Activity in the mPFC

Whether the changes mentioned above in neuronal excitability and synaptic function can alter prefrontal neuronal activity

in vivo is an important question. To address it, we utilized calcium imaging, which is widely used to track neural activities over a long time course. We utilized our home-built 3-photon microscope system, which can achieve high-resolution imaging quality at about 1200 μm depth, allowing visualization of the dorsal prelimbic region of the mPFC (Figure 4A). The average laser power was kept under 50 mW for imaging at a depth of ~ 1200 μm , which is far below the limit for causing tissue damage at the brain surface with 3-photon excitation (~ 129 mW) (30).

In vivo calcium activity recordings were carried out in head-fixed, awake mice during nontask resting states during adolescence and adulthood consistent with the time courses mentioned above (Figure 4A). Images were acquired on 3 saline and 4 CNO mice. Representative traces of selected ROIs are shown in Figure 4B, and calcium events are shown in Figure 4C. In adolescence, the frequency of calcium events in the CNO group significantly decreased compared with those in the saline group in adolescence but not adults (Figure 4D). However, the amplitude of calcium events was significantly decreased in the CNO group in adults (Figure 4E). Additionally, the correlation of cell pairs in the CNO group significantly decreased in adolescents but increased in adults (Figure S1), indicating dys-synchronized PN activities in CNO-treated mice. Together, our results indicate that transient MD inhibition in early adolescence leads to a long-term decrease in spontaneous network activity in both adolescence and adulthood, inducing hypofrontality and desynchronization.

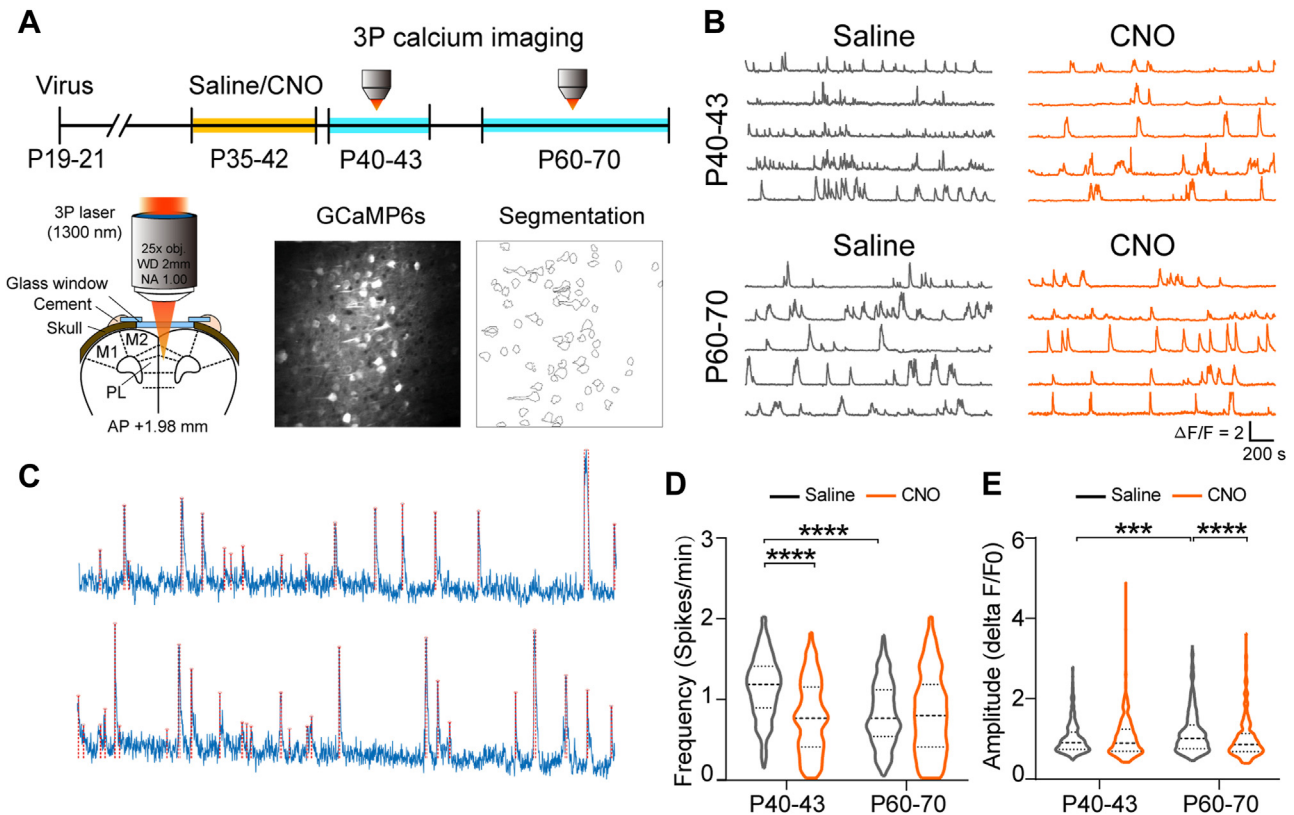


Figure 4. Adolescent mediodorsal thalamus inhibition leads to a reduction of calcium activity of neurons in the mPFC. **(A)** Top: Experimental timeline of in vivo calcium imaging. Bottom left: Schematic of in vivo 3P laser calcium imaging reaching the mPFC at $>1100 \mu\text{m}$ depth. Mice were head fixed and awake during the imaging process. Bottom middle: Average image of mPFC neurons expressing GCaMP6s at $1200 \mu\text{m}$ depth. Bottom right: Segmentation was performed to extract ROIs for calcium activity measurement. **(B)** Representative traces of calcium activities in prefrontal neurons in each group. **(C)** Examples of event detection on normalized traces. **(D)** Frequencies of calcium activities in mHz (event numbers/minute) (P40–P43: saline, $n = 379$ cells; CNO, $n = 386$ cells; P60–P70: saline, $n = 469$ cells; CNO, $n = 320$ cells). Mann-Whitney test, P40–P43: saline vs. CNO, $U = 39,679$, $p < .0001$. Saline: P40–P43 vs. P60–P70: $U = 48,037$, $p < .0001$. **(E)** The amplitude was calculated by averaging the delta F/F_0 of every event in each ROI (2-way analysis of variance, $F = 8.687$, $p < .0001$). Multiple comparisons, saline: P40–P43 vs. P60–P70, $t = 4.236$, $p < .001$; P60–P70, saline vs. CNO, $t = 4.165$, $p < .0001$. **** $p < .0001$, *** $p < .001$. 3P, 3-photon; AP, action potential; CNO, clozapine *N*-oxide; mPFC, medial prefrontal cortex; NA, numerical aperture; P, postnatal day; PL, prelimbic area; ROI, region of interest; WD, working distance.

SST- and PV-INs in the PFC Display Cell Type-Specific Changes

MD afferents also drive feedforward inhibition in the mPFC by targeting INs (18,31). SST- and PV-INs are the 2 largest IN subpopulations in the neocortex. We asked whether adolescent MD inhibition causes long-term effects on membrane excitability in these 2 subtypes of INs. We discovered a cell type-specific change of excitability of layer 2/3 INs in the mPFC. Specifically, in adolescents, SST-INs in the CNO group showed a trending higher firing rate at smaller current steps but a lower firing rate at larger current steps than the saline group (Figure 5A, B). This phenomenon did not last into adulthood. Surprisingly, the firing rate of PV-INs was not affected by MD inhibition in either age group (Figure 5C, D).

We also found that the AMPA/NMDA ratio was significantly increased in SST-INs in adolescence in the CNO group, reaching a value comparable to those seen in adult animals (Figure 6A, B). The PPR and tau of AMPA- and

NMDA-EPSCs were unaffected by CNO treatment (Figure S2). Additionally, we found no changes in the AMPA/NMDA ratio in PV-INs (Figure 6C, D), despite changes in PPR and tau in AMPA-EPSCs (Figure S3). These results suggest that 5-day MD inhibition during early adolescence was insufficient to cause long-lasting changes in excitability and synaptic properties in SST- and PV-INs in the mPFC.

DISCUSSION

Adolescence is a critical period for mPFC maturation during which it is more vulnerable to physiological and environmental changes, including long-range afferent perturbations (32–34). Thalamic inputs are essential for the maturation of circuit organization in the mPFC (35). Our findings demonstrate that adolescent thalamic activity is crucial for mice to respond appropriately to social interactions in adulthood. The most important findings of this study include the observed impaired excitability in both MD and mPFC

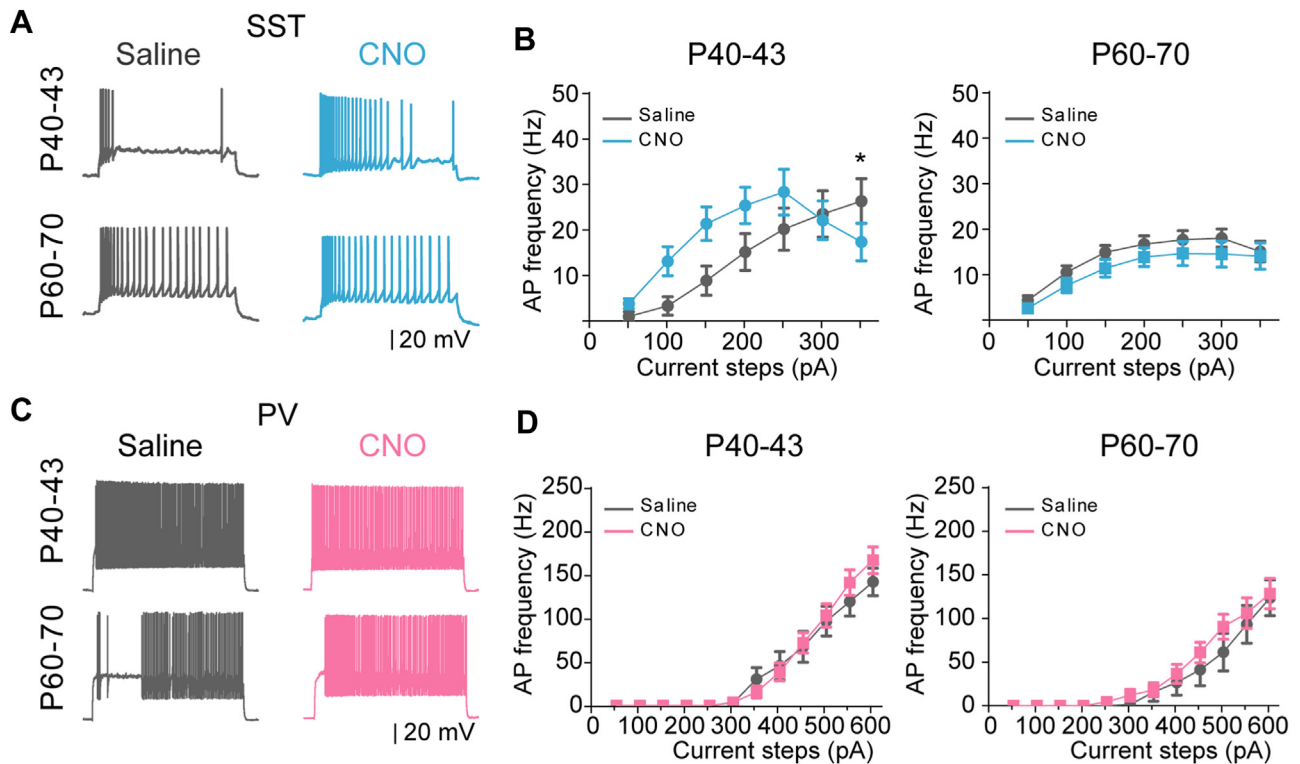


Figure 5. Interneurons in the medial prefrontal cortex show subtype-specific changes in AP frequency. **(A)** Representative traces of APs in SST-INs (200 pA, 1500 ms in duration). **(B)** Curves of AP frequency of SST-INs plotted against input current on P40 to P43 and P60 to P70 [P40–P43: saline, $n = 9$ cells; CNO, $n = 8$ cells; mixed model 2-way analysis of variance, $F_{\text{interaction}(7,105)} = 7.719$, $p < .0001$; multiple comparison, 350 pA, $t = 3.106$, $p = .0188$; P60–P70: saline, $n = 16$ cells; CNO, $n = 12$ cells; $F_{\text{interaction}(7,182)} = 0.3643$, $p = .9219$; $F_{\text{treatment}(1,26)} = 1.235$, $p = .2766$]. **(C)** Representative traces of APs in PV-INs (450 pA, 1500 ms in duration). **(D)** Curves of AP frequency of PV-INs plotted against input current on P40 to P43 and P60 to P70 [P40–P43: saline, $n = 14$ cells; CNO, $n = 15$ cells; mixed model 2-way analysis of variance, $F_{\text{interaction}(12,324)} = 1.225$, $p = .2642$; $F_{\text{treatment}(1,27)} = 0.2880$, $p = .5959$; P60–P70: saline, $n = 12$ cells; CNO, $n = 14$ cells; $F_{\text{interaction}(12,288)} = 0.4538$, $p = .9397$; $F_{\text{treatment}(1,24)} = 0.5571$, $p = .4267$]. * $p < .05$. AP, action potential; CNO, clozapine *N*-oxide; IN, interneuron; P, postnatal day; PV, parvalbumin; SST, somatostatin.

neurons accompanied by deficits in excitatory synaptic transmission and calcium activity in the mPFC, suggesting hypofrontality, together with social memory deficits.

A recent study reported long-lasting impairments in cognitive performance and network excitability in the mPFC following extended MD inhibition (30 days), spanning the

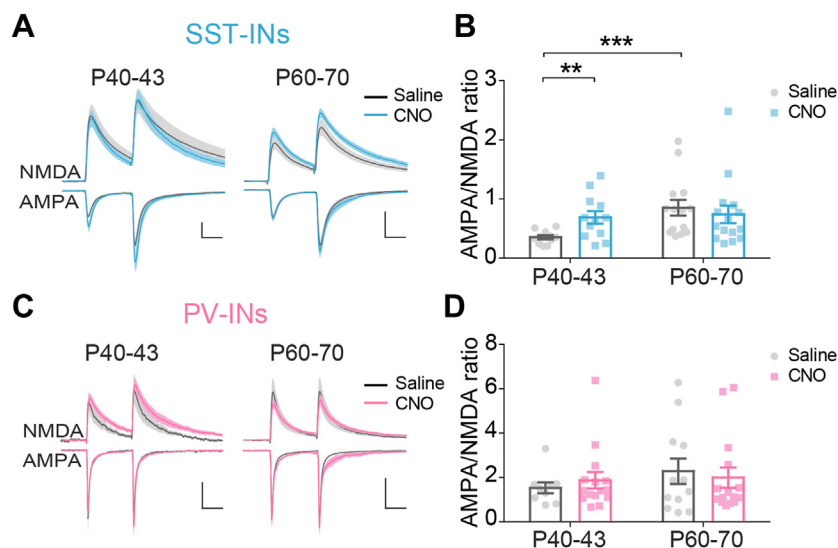


Figure 6. Adolescent mediadorsal thalamus inhibition leads to AMPA/NMDA ratio change in SST-INs but not PV-INs in the medial prefrontal cortex. **(A)** Representative traces showing evoked AMPA and NMDA EPSCs recorded in SST-INs. Scale bar = 50 pA, 50 ms. **(B)** The AMPA/NMDA ratios in SST-INs (P40–P43: saline, $n = 11$ cells; CNO, $n = 12$ cells; P60–P70: saline, $n = 14$ cells; CNO, $n = 15$ cells. Mann-Whitney test as data did not pass the normality test, P40–P43: saline vs. CNO, $U = 23.0$, $p = .007$; saline: P40–P43 vs. P60–P70, $U = 16.0$, $p = .0004$). **(C)** Representative traces of evoked AMPA and NMDA-EPSCs in PV-INs. Scale bar = 50 pA, 50 ms. **(D)** AMPA/NMDA ratios in PV-INs (P40–P43: saline, $n = 9$ cells; CNO, $n = 15$ cells; P60–P70: saline, $n = 12$ cells; CNO, $n = 15$ cells. Mann-Whitney test as data did not pass the normality test, $p > .05$ for all). ** $p < .01$, *** $p < .001$. CNO, clozapine *N*-oxide; EPSC, excitatory postsynaptic current; IN, interneuron; P, postnatal day; PV, parvalbumin; SST, somatostatin.

Adolescent MD Inhibition Induces PFC Deficit in Adults

juvenile-to-late adolescent period (22). Our results further support these findings, demonstrating that even brief thalamocortical disruption (5 days) during adolescence can drive significant electrophysiological and behavioral changes, including persistent impairment in mPFC excitability and synaptic transmission. These findings support a potential foundation for hypofrontality and desynchronization in adulthood, as observed in psychiatric disorders (36–38).

Furthermore, we found that the normal development of social behavior was also associated with MD input-driven mPFC maturation. Numerous studies have demonstrated that inhibiting MD excitatory inputs to the mPFC impairs working-memory performance in both rats (23) and mice (16,22,38,39). While the precise role of the MD and related circuits in social cognition and its development remains unclear. The anterior cingulate cortex–MD circuit plays important roles in modulating prosocial behaviors (40), and the PFC-reuniens circuit is essential for social coding (41). These findings are consistent with the well-established role of the mPFC in social control (42). Our results highlight the importance of the MD–mPFC pathway in social memory and provide a more comprehensive understanding of the roles of mPFC and MD in social behaviors.

The development of neural excitability and synaptic connectivity is highly dependent on the input activity (43). The MD is a major upstream regulator of mPFC activity. We found that neuronal excitability in both thalamic and prefrontal neurons was sensitive to MD activity during adolescence, with adolescent MD inhibition resulting in decreased AP firing frequency in both regions. Our findings demonstrate that even briefer inhibition of MD thalamic activity during adolescence can significantly influence the excitability of the mPFC, contributing to hypofrontality.

Accumulating evidence implicates synaptic plasticity impairment in many psychiatric disorders (44–46). In patients with schizophrenia (SZ), synaptic transmission efficiency and synapse number in layer 2/3 of the PFC are significantly reduced (11,47,48). The onset of this process is triggered by various factors, including perturbation of thalamic input activity in adolescence or early adulthood (48,49). We found that suppressing thalamic activity significantly decreased the AMPA/NMDA ratio in PFC PNs in adolescence and adulthood. This finding implies that MD activity is crucial for the normal development of receptor components in excitatory synapses in the PFC, which may largely contribute to its computational capacity during social cognition.

Next, using calcium imaging, we found that adolescent MD inhibition reduced the amplitude of calcium activity in adulthood, suggesting a reduced spiking activity in the resting state. This finding is consistent with the *ex vivo* electrophysiological results, which revealed long-lasting decreased neuronal excitability and reduced synaptic transmission in adolescents and adults. Cell-pair correlation was significantly decreased in adolescents due to the dramatic short-term reduction of calcium activity in the intact mPFC network after MD inhibition. In adulthood, we observed the opposite changes; the correlation was increased in the CNO group compared with the saline group. The correlation of activities between cell pairs may hint at the synchronization of the

network. While higher correlation suggests more synchronized network activity, oversynchronization may sacrifice the network's flexibility in dynamically encoding information. It was reported in a recent publication that the mPFC ensembles dynamically encode social information with a small group of neurons switching between ON and OFF status during social exploration (50). The increased correlation in our findings may lead to impairment in social cognition due to a decrease in the network dynamics. We found significant social memory impairments in the CNO-treated group, supporting our postulation. However, more experiments are needed to directly test the neural activity changes in the mPFC during social behaviors.

In the last few decades, the importance of GABAergic INs in cognition and psychiatric diseases has been widely studied. Consistent evidence of defects in GABA transmission in the PFC has been found in both patients with SZ and animal models (48,51,52). In postmortem studies, reduced expression of SST and PV messenger RNA has been reported in the dorsolateral PFC of patients with SZ (53,54). However, our results demonstrated differential responses of SST- and PV-INs to thalamic inhibition in adolescence, with the neuronal excitability of SST-INs transiently increased in adolescents and no detectable change in PV-INs. Similarly, the AMPA/NMDA ratio in SST-INs was increased at the same time point. These changes in SST-INs may contribute to the reduction in calcium activity frequency seen *in vivo* in adolescents.

Previous studies have demonstrated the importance of PV-INs in the maturation of prefrontal circuits (55). Suppressing PV-IN activity during adolescence causes persistent impairment in the network activity of the PFC and behavioral flexibility in the set-shifting test. Interestingly, our study found that PV-INs showed a high level of resilience to transient adolescent MD inhibition. The AP frequency was not impacted by transient MD inhibition in adolescence. This evidence suggests that MD activity may not be an upstream driving force in the PV-IN-dependent maturation of the PFC, despite the fact the PV-INs in the PFC receive direct input from the MD. We postulate that the relatively low AMPA/NMDA ratio seen in PV-INs may impart increased resilience to physiological environment perturbation in these cells (15,56).

Conclusions

Developmental disturbances in the mPFC are implicated in social deficits seen in multiple psychiatric disorders. Understanding the normal developmental processes of the mPFC will help identify its vulnerable components, thereby informing future research and potential treatment strategies. We conclude that MD activity in adolescence is critical for maintaining normal excitability and synaptic properties in PNs during adulthood. Furthermore, these changes are reflected in the enhancement of SST-IN excitability and reduction of PN excitability and network activity.

Notably, the development of the MD–mPFC pathway is critical for the performance of social cognition, as reflected by changes in performance on behavioral assays following adolescent MD inhibition. This study provides new insights into the pathogenesis of mPFC-associated psychiatric disorders,

highlighting the critical role of MD-mPFC dysconnectivity involved in hypofrontality.

ACKNOWLEDGMENTS AND DISCLOSURES

This work was supported by the National Institutes of Health (Grant Nos. NIHR21MH110678 and NIHR01MH085666 [to W-JG]); National Natural Science Foundation of China (Grant Nos. T2241002 and 32130044 [to YS]); National Natural Science Foundation of China (Grant No. T2222006 [to BL]); Shanghai Municipal Science and Technology Major Project, Shanghai Pilot Program for Basic Research from Fudan University at China (Grant No. 21TQ1400100/22TQ019 [to BL]); and an award from the Brain Science Interdisciplinary Integration Exploration Project from Fudan University Ministry of Education (MOE) Frontiers Center of China (to BL).

S-SY and W-JG were responsible for conceptualization. S-SY, QH, XG, SL, and WK were responsible for methodology. S-SY was responsible for investigation. S-SY and WK were responsible for visualization. BL, YS, and W-JG were responsible for supervision. SS-Y was responsible for writing the original draft of the article. S-SY, BL, YS, and W-JG were responsible for reviewing and editing the article.

We thank Y.C. Li for guidance and suggestion on patch clamp recordings; A.A. Coley and B. Xing for constructive suggestions on the project design; X. Zhang, S. Deng, and S. Lv for helping with animal maintenance; and L.T. Flynn, J.D. Clarin, A.A. Benson, N.N. Bouras, and V.M. Migovich for editing and commenting on the article.

All data are available in the main text or the [Supplement](#).

The authors report no biomedical financial interests or potential conflicts of interest.

ARTICLE INFORMATION

From the Department of Neurology, Jinshan Hospital, State Key Laboratory of Medical Neurobiology, Institute for Translational Brain Research, MOE Frontiers Center for Brain Science, MOE Innovative Center for New Drug Development of Immune Inflammatory Diseases, Fudan University, Shanghai, China (S-SY, QH, SL, WK, BL, YS); Department of Neurobiology and Anatomy, Drexel University College of Medicine, Philadelphia, Pennsylvania (S-SY, W-JG); and Department of Neurosurgery, Huashan Hospital, Fudan University, Shanghai, China (S-SY, XG, LC, BL).

Address correspondence to Wen-Jun Gao, M.D., Ph.D., at wj38@drexel.edu, Yousheng Shu, Ph.D., at Yousheng@fudan.edu.cn, or Bo Li, Ph.D., at bo_li@fudan.edu.cn.

Received Jan 3, 2025; revised Mar 4, 2025; accepted Mar 10, 2025.

Supplementary material cited in this article is available online at <https://doi.org/10.1016/j.bpsgos.2025.100486>.

REFERENCES

- Koukoulis F, Rooy M, Tziotis D, Sailor KA, O'Neill HC, Levenga J, *et al.* (2017): Nicotine reverses hypofrontality in animal models of addiction and schizophrenia. *Nat Med* 23:347–354.
- Barch DM, Carter CS, Braver TS, Sabb FW, MacDonald A, Noll DC, Cohen JD (2001): Selective deficits in prefrontal cortex function in medication-naïve patients with schizophrenia. *Arch Gen Psychiatry* 58:280–288.
- Arnsten AF (2009): The emerging neurobiology of attention deficit hyperactivity disorder: The key role of the prefrontal association cortex. *J Pediatr* 154:l-s43.
- Courchesne E, Mouton PR, Calhoun ME, Semendeferi K, Ahrens-Barbeau C, Hallet MJ, *et al.* (2011): Neuron number and size in prefrontal cortex of children with autism. *JAMA* 306:2001–2010.
- Stigler KA, McDonald BC, Anand A, Saykin AJ, McDougle CJ (2011): Structural and functional magnetic resonance imaging of autism spectrum disorders. *Brain Res* 1380:146–161.
- Billeke P, Aboitiz F (2013): Social cognition in schizophrenia: From social stimuli processing to social engagement. *Front Psychiatry* 4:4.
- Qin L, Ma K, Wang ZJ, Hu Z, Matas E, Wei J, Yan Z (2018): Social deficits in Shank3-deficient mouse models of autism are rescued by histone deacetylase (HDAC) inhibition. *Nat Neurosci* 21:564–575.
- Green MF, Wynn JK, Eisenberger NI, Horan WP, Lee J, McCleery A, *et al.* (2024): Social cognition and social motivation in schizophrenia and bipolar disorder: Are impairments linked to the disorder or to being socially isolated? *Psychol Med* 54:2015–2023.
- Novak L, Malinakova K, Trnka R, Mikoska P, Sverak T, Kiiski H, *et al.* (2024): Neural bases of social deficits in ADHD: A systematic review. Does the theory of mind matter? *Brain Res Bull* 215:111011.
- Carpenter Rich E, Loo SK, Yang M, Dang J, Smalley SL (2009): Social functioning difficulties in ADHD: Association with PDD risk. *Clin Child Psychol Psychiatry* 14:329–344.
- Forsyth JK, Lewis DA (2017): Mapping the consequences of impaired synaptic plasticity in schizophrenia through development: An integrative model for diverse clinical features. *Trends Cogn Sci* 21:760–778.
- Wamsley B, Fishell G (2017): Genetic and activity-dependent mechanisms underlying interneuron diversity. *Nat Rev Neurosci* 18:299–309.
- Moreau AW, Kullmann DM (2013): NMDA receptor-dependent function and plasticity in inhibitory circuits. *Neuropharmacology* 74:23–31.
- Gonzalez-Burgos G, Miyamae T, Nishihata Y, Krimer OL, Lewis DA (2023): Strength of excitatory inputs to Layer 3 pyramidal neurons during synaptic pruning in the monkey prefrontal cortex: Relevance for the pathogenesis of schizophrenia. *Biol Psychiatry* 94:288–296.
- Gao W-J, Yang S-S, Mack NR, Chamberlin LA (2022): Aberrant maturation and connectivity of prefrontal cortex in schizophrenia: Contribution of NMDA receptor development and hypofunction. *Mol Psychiatry* 27:731–743.
- Bolkan SS, Stujenske JM, Parnaudeau S, Spellman TJ, Rauffenbart C, Abbas AI, *et al.* (2017): Thalamic projections sustain prefrontal activity during working memory maintenance. *Nat Neurosci* 20:987–996.
- Hoover WB, Vertes RP (2007): Anatomical analysis of afferent projections to the medial prefrontal cortex in the rat. *Brain Struct Funct* 212:149–179.
- Åhrlund-Richter S, Xuan Y, van Lunteren JA, Kim H, Ortiz C, Pollak Dorocic I, *et al.* (2019): A whole-brain atlas of monosynaptic input targeting four different cell types in the medial prefrontal cortex of the mouse. *Nat Neurosci* 22:657–668.
- Laubach M, Amarante LM, Swanson K, White SR (2018): What, if anything, is rodent prefrontal cortex? *eNeuro* 5:ENEURO.0315-18.2018.
- Preuss TM (1995): Do rats have prefrontal cortex? The rose-Woolsey-Akert program reconsidered. *J Cogn Neurosci* 7:1–24.
- Parnaudeau S, Bolkan SS, Kellendonk C (2018): The mediodorsal thalamus: An essential partner of the prefrontal cortex for cognition. *Biol Psychiatry* 83:648–656.
- Benoit LJ, Holt ES, Posani L, Fusi S, Harris AZ, Canetta S, Kellendonk C (2022): Adolescent thalamic inhibition leads to long-lasting impairments in prefrontal cortex function. *Nat Neurosci* 25:714–725.
- Ferguson BR, Gao W-J (2018): Thalamic control of cognition and social behavior via regulation of gamma-aminobutyric acid signaling and excitation/inhibition balance in the medial prefrontal cortex. *Biol Psychiatry* 83:657–669.
- Wang HX, Gao WJ (2012): Prolonged exposure to NMDAR antagonist induces cell-type specific changes of glutamatergic receptors in rat prefrontal cortex. *Neuropharmacology* 62:1808–1822.
- Xing B, Mack NR, Guo KM, Zhang YX, Ramirez B, Yang SS, *et al.* (2021): A subpopulation of prefrontal cortical neurons is required for social memory. *Biol Psychiatry* 89:521–531.
- Li X, Zhang G, Wu J, Zhang Y, Zhao Z, Lin X, *et al.* (2021): Reinforcing neuron extraction and spike inference in calcium imaging using deep self-supervised denoising. *Nat Methods* 18:1395–1400.
- Ray A, Christian JA, Mosso MB, Park E, Wegner W, Willig KI, Barth AL (2023): Quantitative fluorescence analysis reveals dendrite-specific thalamocortical plasticity in L5 pyramidal neurons during learning. *J Neurosci* 43:584–600.
- Tozzi A, Scilip A, Tantucci M, de Iure A, Ghiglieri V, Costa C, *et al.* (2015): Region- and age-dependent reductions of hippocampal long-term potentiation and NMDA to AMPA ratio in a genetic model of Alzheimer's disease. *Neurobiol Aging* 36:123–133.

Adolescent MD Inhibition Induces PFC Deficit in Adults

29. Otmakhova NA, Otmakhov N, Lisman JE (2002): Pathway-specific properties of AMPA and NMDA-mediated transmission in CA1 hippocampal pyramidal cells. *J Neurosci* 22:1199–1207.
30. Redlich MJ, Prall B, Canto-Said E, Busarov Y, Shirinyan-Tuka L, Meah A, Lim H (2021): High-pulse-energy multiphoton imaging of neurons and oligodendrocytes in deep murine brain with a fiber laser. *Sci Rep* 11:7950.
31. Delevich K, Tucciarone J, Huang ZJ, Li B (2015): The mediodorsal thalamus drives feedforward inhibition in the anterior cingulate cortex via parvalbumin interneurons. *J Neurosci* 35:5743–5753.
32. Kolb B, Mychasiuk R, Muhammad A, Li Y, Frost DO, Gibb R (2012): Experience and the developing prefrontal cortex. *Proc Natl Acad Sci USA* 109(suppl 2):17186–17193.
33. Caballero A, Orozco A, Tseng KY (2021): Developmental regulation of excitatory-inhibitory synaptic balance in the prefrontal cortex during adolescence. *Semin Cell Dev Biol* 118:60–63.
34. Yang S, Tseng KY (2022): Maturation of corticolimbic functional connectivity during sensitive periods of brain development. *Curr Top Behav Neurosci* 53:37–53.
35. Ferguson BR, Gao WJ (2014): Development of thalamocortical connections between the mediodorsal thalamus and the prefrontal cortex and its implication in cognition. *Front Hum Neurosci* 8:1027.
36. Anticevic A, Haut K, Murray JD, Repovs G, Yang GJ, Diehl C, *et al.* (2015): Association of thalamic dysconnectivity and conversion to psychosis in youth and young adults at elevated clinical risk. *JAMA Psychiatry* 72:882–891.
37. Woodward ND, Karbasforoushan H, Heckers S (2012): Thalamocortical dysconnectivity in schizophrenia. *Am J Psychiatry* 169:1092–1099.
38. Kupferschmidt DA, Gordon JA (2018): The dynamics of disordered dialogue: Prefrontal, hippocampal and thalamic miscommunication underlying working memory deficits in schizophrenia. *Brain Neurosci Adv* 2:2398212818771821.
39. Parnaudeau S, O'Neill PK, Bolkan SS, Ward RD, Abbas AI, Roth BL, *et al.* (2013): Inhibition of mediodorsal thalamus disrupts thalamo-frontal connectivity and cognition. *Neuron* 77:1151–1162.
40. Song D, Wang C, Jin Y, Deng Y, Yan Y, Wang D, *et al.* (2023): Mediodorsal thalamus-projecting anterior cingulate cortex neurons modulate helping behavior in mice. *Curr Biol* 33:4330–4342.e5.
41. Chen Z, Han Y, Ma Z, Wang X, Xu S, Tang Y, *et al.* (2024): A prefrontal-thalamic circuit encodes social information for social recognition. *Nat Commun* 15:1036.
42. Anderson DJ (2016): Circuit modules linking internal states and social behaviour in flies and mice. *Nat Rev Neurosci* 17:692–704.
43. Andreae LC, Burrone J (2018): The role of spontaneous neurotransmission in synapse and circuit development. *J Neurosci Res* 96:354–359.
44. Otto LR, Clemens V, Üsekes B, Cosma NC, Regen F, Hellmann-Regen J (2023): Retinoid homeostasis in major depressive disorder. *Transl Psychiatry* 13:67.
45. Kawabata R, Yamanaka H, Kobayashi K, Oke Y, Fujita A, Oku Y, *et al.* (2023): The anterior cingulate cortex is critical for acute stress-induced hypersensitivity in mice. *Neuroscience* 523:47–60.
46. Winzenried ET, Everett AC, Saito ER, Miller RM, Johnson T, Neal E, *et al.* (2023): Effects of a true prophylactic treatment on hippocampal and amygdala synaptic plasticity and gene expression in a rodent chronic stress model of social defeat. *Int J Mol Sci* 24:11193.
47. Selemon LD, Goldman-Rakic PS (1999): The reduced neuropil hypothesis: A circuit based model of schizophrenia. *Biol Psychiatry* 45:17–25.
48. Selemon LD, Zecevic N (2015): Schizophrenia: A tale of two critical periods for prefrontal cortical development. *Transl Psychiatry* 5:e623.
49. Paus T, Keshavan M, Giedd JN (2008): Why do many psychiatric disorders emerge during adolescence? *Nat Rev Neurosci* 9:947–957.
50. Liang B, Zhang L, Barbera G, Fang W, Zhang J, Chen X, *et al.* (2018): Distinct and dynamic ON and OFF neural ensembles in the prefrontal cortex code social exploration. *Neuron* 100:700–714.e9.
51. Benes FM, Berretta S (2001): GABAergic interneurons: Implications for understanding schizophrenia and bipolar disorder. *Neuro-psychopharmacology* 25:1–27.
52. Dienel SJ, Lewis DA (2019): Alterations in cortical interneurons and cognitive function in schizophrenia. *Neurobiol Dis* 131:104208.
53. Morris HM, Hashimoto T, Lewis DA (2008): Alterations in somatostatin mRNA expression in the dorsolateral prefrontal cortex of subjects with schizophrenia or schizoaffective disorder. *Cereb Cortex* 18:1575–1587.
54. Mellios N, Huang HS, Baker SP, Galdzicka M, Ginns E, Akbarian S (2009): Molecular determinants of dysregulated GABAergic gene expression in the prefrontal cortex of subjects with schizophrenia. *Biol Psychiatry* 65:1006–1014.
55. Canetta SE, Holt ES, Benoit LJ, Teboul E, Sahyoun GM, Ogden RT, *et al.* (2022): Mature parvalbumin interneuron function in prefrontal cortex requires activity during a postnatal sensitive period. *eLife* 11: e80324.
56. Wang H-X, Gao W-J (2009): Cell type-specific development of NMDA receptors in the interneurons of rat prefrontal cortex. *Neuro-psychopharmacology* 34:2028–2040.